2. State of the art for field monitoring methods and database for actual energy efficiency of heat pump systems

2.1 Background

As a promising technology for cooling and heating, heat pump has been applied in various commercial buildings, residential buildings and industrial buildings worldwide. According to its configuration, a heat pump can be packaged or split, ducted or ductless, portable or stationary. Typical heat pump types include mini-split system, variable refrigerant flow (VRF) system or multi-split system, packaged window unit, central ducted split system, packaged roof top unit, etc. (IEA, 2019) The global demand forecast for commercial and residential air conditioners in 2022 is estimated to have increased by 107% compared to the previous year, with approximately 17.87 million units for commercial use and 99.9 million units for residential use (JRAIA, 2023). In China, annual production of RACs reaches 218 million units in 2022. Moreover, VRF system has long held the market's largest share for central air conditioning (Central Air Conditioning Market, 2020). The Chinese market's enormous sales volume has aided in the growth of VRFs in the European and American markets.

In the background of the vast market scale, actual performance and energy efficiency of the heat pump system has raised wide attention in recent years. Although heat pump systems exhibit high performance efficiency with various control strategy optimizations in the laboratory, their actual field performance could be much different. Actual operation characteristics are affected by various factors, such as indoor and outdoor environmental parameters, pipe length and installation condition, thermal performance of enclosure structure, occupants' behaviour and so on, which could differ from those in the laboratory. In actual operation, such as short-circuiting in the outdoor unit during cooling, defrost operation during heating, and low-load operation due to excess equipment capacity for claims, avoidance lead to a deviation of energy performance from the values in the catalogue. According to the field test by Won et al. (Won et al. 2009), the actual energy efficiency of the VRF system in cooling season was only 1.74 kWh/kWh, which is remarkably lower than its nominal cooling energy efficiency of 2.64 kWh/kWh. According to the investigation by Matsui et al. (Matsui et al., 2016), the average operating ratio (actual output/nominal output) of VRF system in Japan is approximately 25%. The normalisation of oversized capacity leads to inefficient operation.

Accurate measurement of the cooling and heating capacity becomes the focal point of field performance measurement since the energy efficiency index (EER) for the cooling mode and (COP) for the heating mode could be calculated, respectively, from the energy consumption and capacity. The energy efficiency index such as EER (Energy Efficiency Ratio), SEER (Seasonal Energy Efficiency Ratio), and COP (Coefficient of Performance) are all calculated as the ratio of capacity to energy consumption, making accurate measurement of cooling and heating capacities a crucial focus in on-site evaluations.

Among the different types of heat pump, cooling/heating performance of water-medium ones can be easily measured by measuring the water flow rate and its temperature difference. However, for air-to-air systems, on-field capacity-related performance of the system is hard to be determined, though electricity consumption can be measured (Matsui&Kametani, 2020). As a result, the challenge of performance measurement to air-to-air system impedes the development of energy management, energy-saving operation, system retrofitting.

Thus, this chapter reviews the state of art for field monitoring methods of heat pump systems (mainly focus on air-to-air system) and introduces some measurement result and database for actual performance of heat pump.

2.2 Current field monitoring methods

The cooling or heating capacity can be obtained for water-cooled heat pump systems by measuring the water temperature difference and water circuit flow rate. However, this is not the case for air-to-air heat pump.

2.2.1 Air-air heat pump systems

The basic principle of performance measurement of air-to-air heat pump is presented in Figure 2.2.1-1 (Enteria et al., 2023). In order to obtain the cooling or heating capacity of the air-to-air system, researchers mainly focus on two methodologies according to the measured medium (air or refrigerant), namely the air-specific enthalpy difference (AE) method and refrigerant specific enthalpy difference (RE) method. According to different acquisition methods of air volume and air enthalpy difference, the AE method is further divided into indoor side AE method and outdoor side AE method. The former comprises indoor air hood method and indoor air sampling method, the latter is composed of the outdoor air hood method, static multi-point sampling method, static outlet air sampling method and dynamic outlet air sampling method. Based on a different of refrigerant mass flow measurement principle, the RE method is divided into the refrigerant flowmeter method, compressor performance curve method, compressor volume efficiency method, numerical calculation method and compressor energy conservation method.

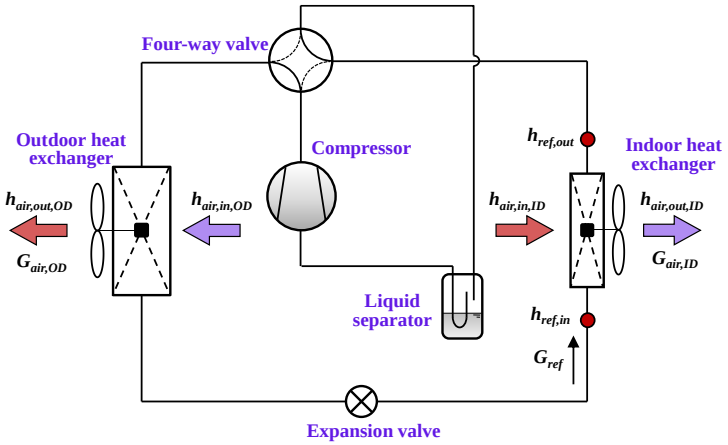

$$\dot{Q}_{cc} = \dot{m}_{air,ID} \cdot \left(h_{air,in,ID} - h_{air,out,ID}\right) \quad = \dot{m}_{air,OD} \cdot \left(h_{air,out,OD} - h_{air,in,OD}\right) - P_{com} \quad = \dot{m}_{ref} \cdot \left(h_{ref,out} - h_{ref,in}\right)$$
$$\dot{Q}_{hc} = \dot{m}_{air,ID} \cdot \left(h_{air,out,ID} - h_{air,in,ID}\right) \quad = \dot{m}_{air,OD} \cdot \left(h_{air,in,OD} - h_{air,out,OD}\right) + P_{com} \quad = \dot{m}_{ref} \cdot \left(h_{ref,in} - h_{ref,out}\right)$$

Indoor air side | Outdoor air side | Refrigerante side

Figure 2.2.1-1. Basic principle of field performance measurement to air-to-air heat pump

2.2.1.1 Indoor side air enthalpy difference method

The indoor side air enthalpy difference method mainly includes the indoor unit external air hood and the indoor unit outlet air sampling method. The external method is based on the traditional heat transfer measurements on the air side, mainly air flow rate, inlet and outlet temperature, and corresponding air properties, such as density and specific heat capacity. The air flow rate can be measured directly by anemometer or calculated according to a fan curve validated by experiments, such as a function among air flow rate, fan rotation speed and power consumption.

2.2.1.1.1 Air hood method

The air hood introduces all the air outlets of the indoor unit into the air duct, and the fan adjusts its speed at the end of the air duct to balance the pressure loss caused by the test devices at the same time (Jactard&Li, 2011). The anemometer and the temperature/humidity sensors were used to obtain the air volume and the parameters before and after the heat exchanger. In addition, at least four groups of temperature and humidity sensors should be installed in the inlet and outlet of the indoor unit evenly distributed. To obtain accurate air density and specific heat capacity, a group of temperature and humidity sensors shall be arranged near the pressure sensor. Although use of multiple groups of temperature and humidity reduces the error caused by thermal non-uniformity, it is not convenient because it disturbs the regular operation for both users and units.

2.2.1.1.2 Air sampling method

To simplify the test difficulties, the air sampling method was proposed. The indoor unit's inlet and outlet distribution is determined through multi-point measurement in advance; therefore, the air hood could be left out in the field test. The inlet and outlet areas are normally divided into several small regions, and the air temperature, humidity, and velocity are measured, respectively.

Figure 2.2.1-2 shows the test principle of an indoor unit of a multi-connected air conditioner of a four-side air outlet ceiling unit (Ichikawa et al., 2008). The scalar and vector anemometer measured three-dimensional airflow velocities in and from the unit, creating an accurate airflow velocity distribution curve. The air inlet and outlet volumes are calculated by integrating distributed sensors and each measuring point´s correction factor. The temperature and humidity sensors are arranged in each measuring point area. Therefore, the cooling capacity was finally obtained.

Figure 2.2.1-3 shows the thermal and vector velocity distribution in the indoor unit, where the airflow at the outlet is also complex, similar to the outdoor unit. Ensuring this method´s accuracy is hard, especially in the cooling condition. Moreover, using the arithmetical average should be avoided since the supply air exhibits evident non-uniformity.

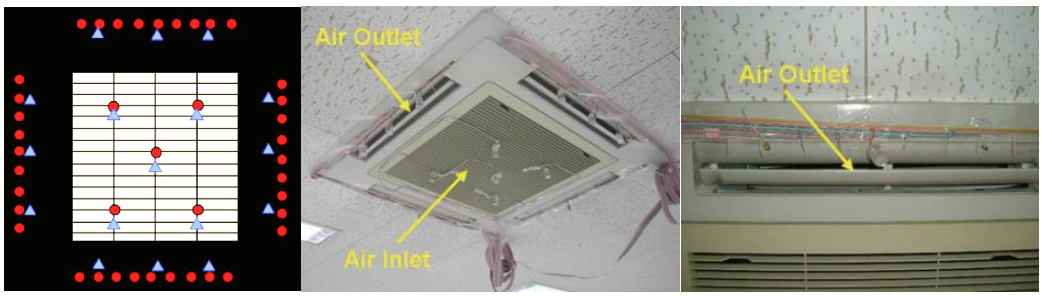

(a) Measuring point (b) Air inlet and outlet (c) Sensors of air outlet

Figure 2.2.1-2. Air sampling method

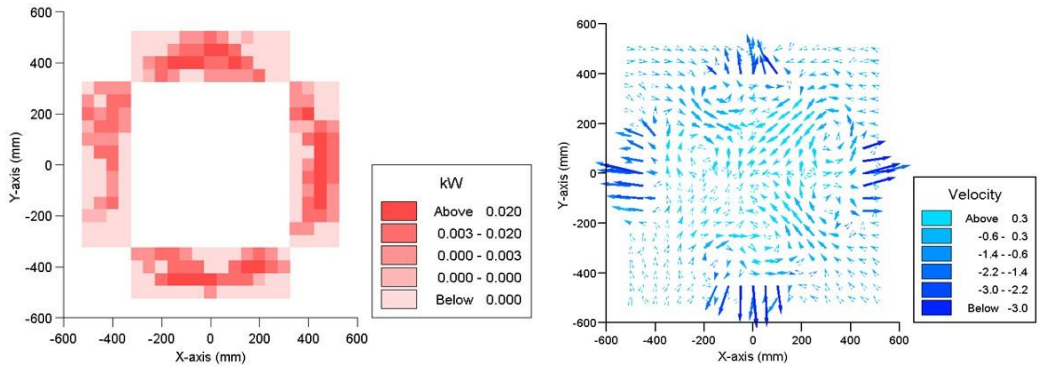

Figure 2.2.1-3. Thermal and vector velocity distribution on the indoor unit

2.2.1.2 Outdoor side air enthalpy difference method

Although the indoor air enthalpy difference method has the advantage of being free from the interference of outdoor meteorological conditions, it is difficult to achieve high-precision long-term measurement due to its interference from the users.

2.2.1.2.1 Static multi-point air sampling method

The cooling/heating capacity was calculated by multiplying the enthalpy difference and the air mass flow rate in the static multi-point air sampling method. The specific enthalpy is calculated by arranging several groups of temperature and humidity sensors at the inlet and outlet of the outdoor unit. Similarly, the air volume was determined by measuring air speed in multiple positions of the outdoor unit. Probing temperature sensors show better accuracy since they penetrate the heat exchanger and the synchronisation (Nobe et al., 2011). Each probing sensor is equipped with two T-type thermocouples, one of which is put on the exterior of heat exchange fins, and the other penetrates through fins into exhaust air chambers so that the inlet and outlet temperature of the heat exchanger can be measured at one time. In the field test, Ichikawa et al. (Ichikawa et al., 2008) tested the performance of the air source heat pump with a large capacity installed in an office building in central Tokyo by 27 probing sensors. The velocity of exhaust airflow was measured on each fan unit.

2.2.1.2.2 Air hood method

The air hood is connected to the air outlet of the outdoor unit (Shimuzu et al., 2006), similar to the indoor air hood method. The average inlet/outlet air parameters (temperature and humidity) and airspeed distribution were measured and calculated. Compared with the air sampling method, the interference of the outdoor environment is avoided with better airflow uniformity.

A rectangular duct is set at the air outlet of the outdoor unit to measure heat exchange by temperature and humidity sensor. Figure 2.2.1-4 shows the outdoor unit´s duct part and vector velocity distribution. The airflow within the duct is a swirling flow. Velocity components primarily influence the thermal distribution and make accurate measurements challenging.

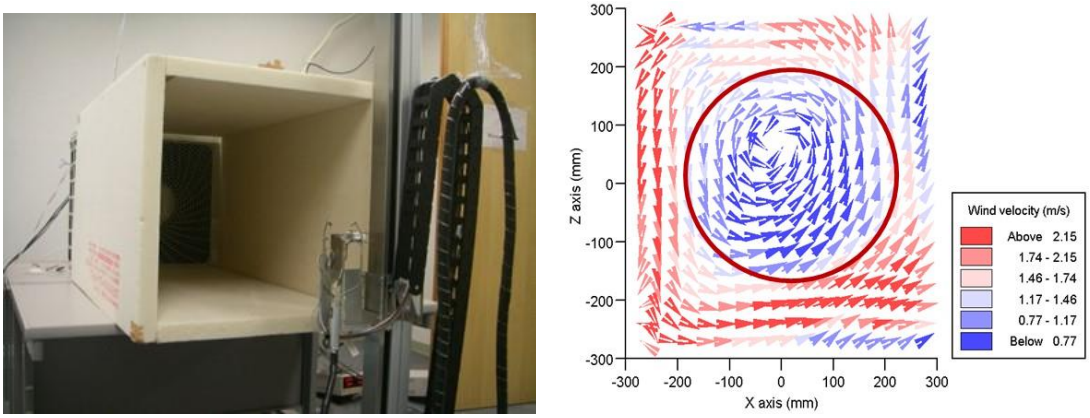

Figure 2.2.1-4. Duct in the outdoor unit and vector velocity distribution

However, installing an air hood affects the air distribution of the air flow field of outdoor units, especially for the multiple outdoor units. The relative error of this method is about ±15%.

2.2.1.2.3 Static outlet air sampling method

By installing of air outlet sampling devices at the outlet of the outdoor unit, the sampling devices obtain the temperature, humidity, and airflow parameters at the microelement (Shimuzu et al., 2007). In order to improve the accuracy, the cooling capacity algorithm was improved. A sampling device that samples the exhaust heat from an outdoor unit was developed by Haga et al. (Haga et al., 2007), which was called the thermal flux sampler. An illustration of the thermal flux sampler is shown in Figure 2.2.1-5. The average mean error was 12% compared with the heat balance method, which shows a great improvement in

evaluating the actual performance of the VRF system. However, considering the complex structure of the measuring device, the installation of the measuring device is complex. In addition, it is necessary to introduce the outlet angle and flow correction coefficient, showing with significant uncertainties.

2.2.1.2.4 Dynamic outlet air sampling method

To solve the problems of difficult installation and complex debugging of the outdoor unit static outlet air sampling method, Zhao (Zhao, 2009) proposed the dynamic outlet air sampling method, which used sensors connected with a rotating rod on a rotating shaft driven by the stepping motor moving at a predetermined speed (Figure 2.2.1.6). The total cooling capacity was obtained by the accumulation of a sub-zone heat transfer.

The mechanical automatic control device complemented the measurement progress, avoiding the anthropic factors' effects. The measurement cost increased significantly for the cost of motor and control devices. Moreover, it is not convenient to install the equipment in some cases, which also restricts the application of this method.

Figure 2.2.1-5. Static outlet air sampling device

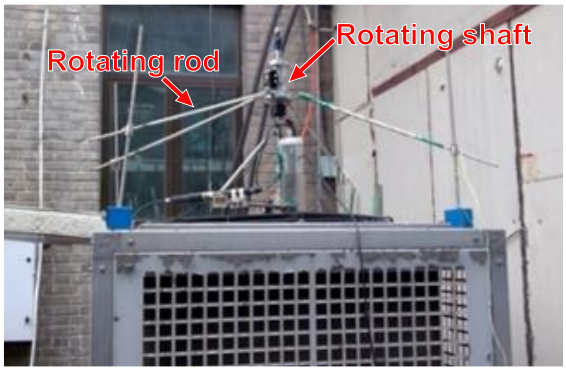

Figure 2.2.1-6. Dynamic outlet air sampling device

2.2.1.3 Refrigerant specific enthalpy difference method

2.2.1.3.1 Compressor performance curve method

Based on the provided information, the compressor performance curve method calculates the refrigerant mass flow rate by fitting a polynomial to some directly measured parameters such as evaporation temperature, condensation temperature, adiabatic compression index and compressor frequency. The polynomial is then applied to the actual operating conditions, and the refrigerant mass flow rate under the corresponding operating conditions is calculated. The cooling/heating capacity of the system is determined by calculating the enthalpy difference between the refrigerant inlet and outlet of the indoor heat exchanger. Related studies prove that the relative errors with approximated and measured refrigerant mass flow rate values are within 6~10% (Takahashi et al., 2008).

However, the compressor performance curve method relies on the fundamental information supplied by the manufacturer. In addition, after the long-term operation, some problems, such as compressor´s wear and tear, and refrigerant leakage, will affect the compressor´s performance. The field performance of the compressor will deviate from the initial performance in the laboratory, showing low accuracy in a long-term test.

2.2.1.3.2 Compressor volumetric efficiency (CVE) method

The ratio of the actual suction volume to the theoretical suction volume is used to define the volumetric efficiency of the compressor (Naruhiro&Shigeki, 2012). As a result, once the volumetric efficiency and structure of the compressor are determined, the refrigerant mass flow rate (or cylinder volume) may be calculated according to Equation (2.2.1.1).

$$\dot{m}_{ref} = \rho_{ref} \times \eta_v \times V_d \times f \tag{2.2.1.1}$$

Where, η_v represents volumetric efficiency, V_d is the actual suction volume of the compressor (m^3/rev), and f represents the frequency of the compressor (Hz). The volumetric efficiency value can be experimentally determined from the air conditioning capacity in a high-precision environmental test laboratory. Figure 2.2.1-7 shows the volumetric efficiency of a scroll compressor obtained using this technique. The error factors and their approximate values for the simplified compressor curve method are shown in Table 2.2.1-1. The total error is over 20%, but since each factor is an independent event, the overall error is within 10%. The disadvantage of the compressor curve method is that the error increases during transient operating conditions, such as when the compressor starts up. However, the error during steady operation is small, and it can be said to be a sufficiently practical evaluation method. In addition, the accuracy of this method depends on the precision of volumetric efficiency, which may be affected by the wear and deterioration of the compressor during a long-term operation.

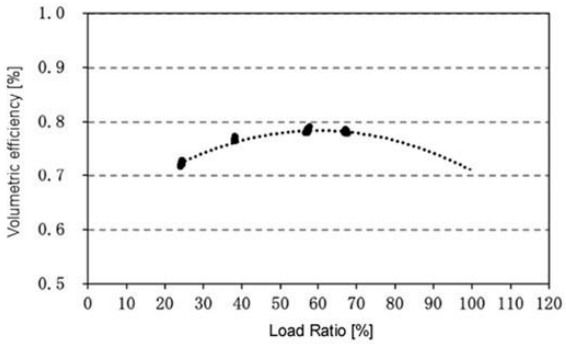

Figure 2.2.1-7. Volumetric efficiency

Table 2.2.1-1. Error factors in the compressor curve method

Causal factors	Individual differences	During operation	
		Cooling	Heating
Variability in Compressor Individual Performance	within ±5%	within ±2.5%	within ±2.5%
Approximation Error in Compressor Performance Characteristics	within ±5%	within ±5%	within ±5%
Four-way valve leakage		within ±0.5%	within ±0.5%
Sensor errors		±0.5% each	±0.5% each
Heat dissipation losses (Liquid piping)		within 2-3%	

2.2.1.3.3 Refrigerant mass flow meters method

The intrusive measurements on the refrigerant side can directly obtain the refrigerant mass flow. Teodorese et al. (Teodorese et al., 2007) determined the refrigerant flow rate by using the Coriolis flow meter installed at the exhaust side of the indoor unit during the heating season. Tran et al. (Tran et al., 2012) used two mass flow meters (Coriolis flow meter and external ultrasonic flow meter) in the laboratory to evaluate the flow rate and vapor quality of the refrigerant. It is shown that the averaged relative error of the method even reaches to 1.8% compared with water enthalpy method during a long period field test. However, the Coriolis flow meter is expensive, and it is inevitably intrusive, which will seriously affect the operation state of a heat pump. In addition, the accuracy of the Coriolis flow meter is significantly reduced when inlet refrigerant is in a two-phase or non-steady state.

2.2.1.3.4 Throttling model method

According to the throttling characteristic equation for a compressible fluid, the Throttling Model Method determines the mass flow rate of the refrigerant based on the compressible fluid throttling characteristic equation. Kim & Braun (2016) investigated three different virtual refrigerant mass flow sensors (VRMF) that use mathematical models to estimate flow rate, including the compressor map method, energy balance method, and empirical correlated throttling model method. According to experiments, the three VRMFs work well in estimating refrigerant mass flow rate for various systems with less than 5% root-mean-square error.

2.2.1.3.5 Compressor energy conservation (CEC) method

First proposed by Fahlén (1989), the compressor energy conservation method measures the refrigerant mass flowrate across the compressor based on the energy conservation equation, shown as Equation (2.2.1.2).

$$\dot{m}_{ref} h_{suc} + P_{com} = \dot{m}_{ref} h_{suc} + \dot{Q}_{loss} \qquad (2.2.1.2)$$

where, m_{ref} represents refrigerant mass flow rate across the compressor, in kg/s; h_{suc} and h_{dis} represent the refrigerant specific enthalpy at compressor suction and discharge port, in kJ/kg; P_{com} represents electric power input, in kW; Q_{loss} represents heat loss between compressor and surrounding, in kW.
For a room air conditioner where the refrigerant mass flow rate across the compressor equals that across all indoor units, the CEC method can be directly applied to obtain the field performance. However, for a VRF system with multiple circuits, such as oil return and subcooling circuits, the refrigerant mass flowrate across the compressor does not necessarily equal to that across all indoor units. In this case, the compressor set energy conservation (CSEC) method is proposed by Zhang et al. (Zhang et al., 2019) to solve this problem. Further, to cope with the two-phase suction situation and increase the method's accuracy, the CEC-CVE method is proposed to improve the measurement accuracy in two-phase suction condition (Yang et al., 2020; Xiao et al., 2022). The accuracy of this method is finally proved to be approximately 15% compared with the AE method. This method shows long-term reliability, independence, and non-interference, which are significant requirements for field tests.

2.2.2 Air-water (hydronic) heat pumps

Previous measurement methods (AE and RE methods) can be applied with similar principles for air-water heat pumps. In addition, the water side method is available for performance measurement cases where the water side is accessible. The water flow rate and temperature can be accurately measured using a mass

flow meter and temperature sensor. Heat transfer of the outdoor unit is determined accurately from the water side by Equation (2.2.2.1). In addition, after measuring the compressor's power consumption, the total cooling capacity is calculated by Equation (2.2.2.2), and the total heating capacity is calculated by Equation (2.2.2.3).

$$\dot{Q}_{out,w} = \dot{G}_w c_{pw}\left(t_{w,in} - t_{w,out}\right) \quad (2.2.2.1)$$

$$\dot{Q}_{in,c} = \dot{Q}_{out,w} - P_{com} \quad (2.2.2.2)$$

$$\dot{Q}_{in,h} = \dot{Q}_{out,w} + P_{com} \quad (2.2.2.3)$$

In summary, the AE and RE methods are available approaches to measure heat pump performance. Among these methods, the CEC method is better for its long-term reliability, independence, and non-interference. In addition, for the short-term measurement of new heat pump products (with slight efficiency deterioration), the CVE method is a practical choice. Thus, combining these two methods to realise high-accuracy measurements for heat pumps during their life-cycle may be a promising approach.

2.3 Existing standards and protocols for monitoring methods for heat pump systems

2.3.1 China's specifications and standards

Standardisation is an important way to promote the development and application of the technology. Previous standards in China for the performance testing of heat pump (mainly refer to RAC and VRF system) mainly concentrate on the operating performance in the laboratory, but there are also corresponding specifications for the measurement of the on-site operating performance.

In the regulation produced by Architectural Services Department of the Hong Kong Special Administrative Region (Architectural Services Department, 2007), it required that the air-conditioning system (including the central air system and split air system) should be tested by air enthalpy method in a short time, and the unit should keep full loads in the steady state. Since this regulation is not dedicated to the field test, related technical schemes are not illustrated in detail.

To promote the CEC method, the standard T/CAS 305-2018 "Specification for measurement of on-site performance parameters of air conditioner" (AQSIQ, 2018) was proposed firstly in China, including calculation formulas, installation positions of sensors, and accuracies & calibrations of measuring devices. For air conditioners without pressure sensors, temperature sensors are used to estimate the evaporation/condensation pressure in CEC method. In addition, APF index reflecting the seasonal performance of the unit specified in the energy efficiency standard (e.g. GB 21455-2013 (AQSIQ, 2013)) are used to evaluate accuracy of the measurement device, as shown in Table 2.3.1-1. Through the measurement under the different operating conditions, the tested APF of measuring devices was compared with the results of the psychometric caloric laboratory APF_{IPME}, and the relative error of the two measurement results δ_{IPME} (calculated by Equation (2.3.1.1)) is adopted as the accuracy evaluation index. Based on the measurement results, the accuracy of the measurement device is classified. APF with a relative error of less than 10% can be regarded as a high-precision field performance measuring device, while a measuring device with a relative error of more than 25% is regarded as unqualified.

Table 2.3.1-1. Accuracy calibration conditions of measuring device

Item		Calibration condition				Test item	Necessity
		Indoor side		Outdoor side			
		DBT	WBT	DBT	WBT		
Cooling	Nominal cooling	27	19	35	24	Nominal cooling	○
						Half cooling	○
						25% cooling	○/△
	Low temperature cooling	27	19	29	—	Low temperature	○
	Low humidity cooling	27	＜16	29	—	Low humidity	△
	Intermittent cooling	27	＜16	29	—	Intermittent cooling	△
	Maximum cooling	32	23	43	26	Maximum cooling	△
	Extreme high-temperature	32	23	48	—	Extreme high-temp.	△
Heating	Nominal heating	20	—	7	6	Nominal heating	○
						Half heating	○
						25% heating	○/△
	Intermittent heating					Intermittent heating	△
	Low-temperature heating	20	≤15	2	1	Low temperature	○
	Extreme low-temperature	20	≤15	-7	-8	Extreme low-temp.	○

Note: ○ represent the necessary item, and △ represent the selected item.

$$\delta_{IPME} = \frac{|APF_{IPME} - APF_S|}{APF_S} \times 100\% \qquad (2.3.1.1)$$

In recent years, VRF systems have been widely used with increasing demands in the market. In China, the standard T/CECS “Technical specification for the retrofitting of multi-connected split air condition system” (C.A. of B. Research, 2019) and standard for T/CECS 846-2021 “Performance testing of heating and air-conditioning system in hot summer and cold winter zone” (C.A. of B. Research, 2021) published by the China Association for Engineering Construction Standardisation aims to determine the method and regulations of VRF renewal and retrofitting. In this standard, four classes were determined when considered renewal and retrofitting, including air condition system function, security, environment, and energy efficiency. To acquire the energy efficiency of heat pump, the indoor AE method was recommended to adopt for the cooling/heating capacity of VRF system. In these two standards, the compressor set energy conservation (CSEC) method is included as an available method. The schematic of sensors installation by CSEC method on VRF system is shown in Figure 2.3.1.1. By testing the temperature, pressure and energy consumption, cooling or heating performance of a VRF is finally calculated. In addition, the waterside heat metering method is also recommended for water source VRF system. Therefore, through the standard for retrofit VRF system, the field test methods and related principles are determined, which contribute to the promotion of high-efficiency VRF system in energy-saving transformation projects.

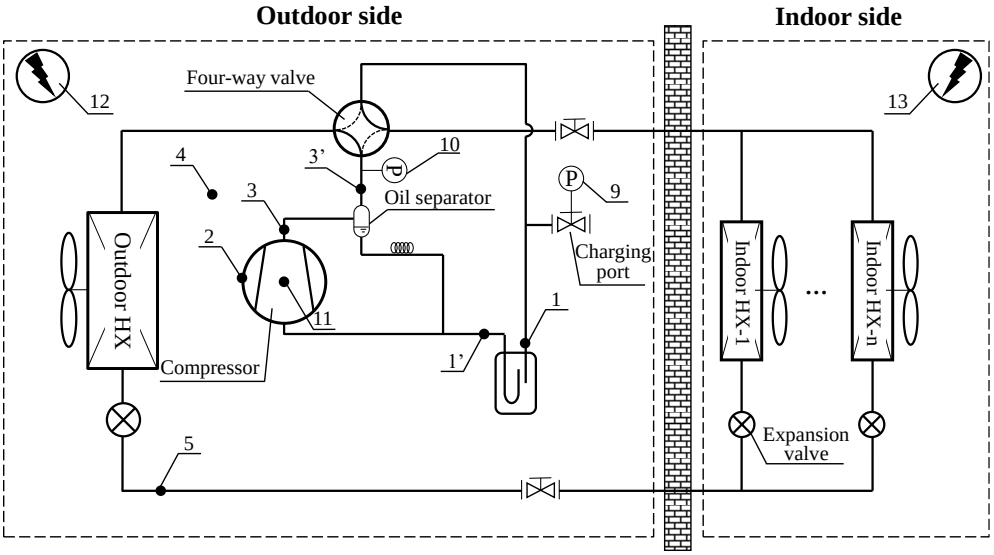

Figure 2.3.1-1. Schematic of sensors installation by CESC method on VRF system

1—Inlet refrigerant temperature of liquid separator；1'— Outlet refrigerant temperature of liquid separator；2—Refrigerat temperature in the middle of compressor (or external insulation)；3—Refrigerant temperature of compressor discharge；3'—Outlet refrigerant temperature of oil separator；4—Outdoor air temperature；5—Inlet(in heating mode) or outlet(in cooling mode) refrigerant temperature of outdoor heat exchanger； 9—Inlet pressure of liquid separator；10—Discharge pressure of compressor；11—Compressor input power；12—Energy consumption recorded by outdoor energy meter；13—Energy consumption recorded by indoor energy meter

In China, performance measurements of heat pumps are receiving increasing attention. Standards incorporating performance measurement techniques currently under development also include T/CECS "Standard for field measurement of energy efficiency and energy saving of multi split air conditioning (heat pump) system" and GB/T 27941 "Code of design and installation for multi split air conditioning (heat pump) system". To verify the consistent accuracy of the performance measuring device during the test, the former one proposed the calibration method under continuous dynamic condition. In addition, The GB/T 27941 standard (Chinese Standards, 2011), which is under revision, plans to apply performance measurement methods to test the effectiveness and acceptance of installed VRF systems.

2.3.2 Canada's specifications

In 2020-2022, Natural Resources Canada funded field trials of air to air, variable capacity cold climate heat pumps in locations across Canada. To provide guidance for these field tests, a technical guideline for field monitoring was developed (Natural Resources Canada, 2022). The Guideline covers 4 planning and undertaking field monitoring aspects, including site and equipment selection, monitoring parameters, short-term testing and long-term testing.

In the first aspect of site and equipment selection, basic information is collected and reported, such as geographical location, house description and use, house heat load, heating and cooling system configuration, system sizing calculations and other details.

In the second aspect, parameters and accuracy in the testing are regulated. Required data mainly includes: whole-house power/energy, system power/energy of outdoor unit and indoor unit(s), backup heat power/energy for the area being heated by the ASHP, outdoor air temperature and humidity, indoor air temperature and humidity, location of outdoor unit, supply and return air temperature, relative humidity at return and supply, indoor unit air flow rate, ventilation air flowrates and temperatures, system runtime during the measurement interval, any unit controls, sensors, or outputs that can be accessed and recorded.

In short-term testing, HP system is set to provide maximum cooling or heating depending on the season. The above parameters are monitored, and the supply air flow rate is calculated according to the fan curve.

The efficiency of HP is measured according to the indoor side AE difference method. The tested capacity, power consumption, and supply conditions are compared with manufacturer submittals or engineering data sheets. The monitoring measurements, when applied correctly, are expected to result in load calculations that are accurate within ±20%, compared to manufacturer data. If any measured performance value is more than 20% off the expected value, double-check sensor performance.
In long-term testing, performance of HP is measured in similar method during a long term. During the testing, periods when the heat pump are off, standby and active mode (cycling on and cycling off) should be recorded to see how well the heat pump matches the heating load of the house. In “Active mode”: the heat pump is the selected heating/cooling system (switched ON) and provides heat/cooling in cycling on or cycling off state. In “Standby mode”: the heat pump is the selected heating system (switched ON) and not providing the heat, as there is no cooling or heating load. In “Off mode”: the heat pump is not the selected heating system (switched OFF) and not providing the heat, but draws electricity.
By counting the temperature bin hours, seasonal performance factor is calculated. For example, Seasonal Coefficient of Performance Calculations in heating season ($SCOP_H$) should be calculated according to Equation (2.3.2.1).

$$SCOP_H = \frac{\sum_{j=1}^{n} \left[Load(T_j) \cdot \frac{j}{N}\right]}{\sum_{j=1}^{n} \left\{\left[\frac{Capacity(T_j)}{COP(T)} + Aux(T_j)\right]\frac{n_j}{N}\right\} + P_{HNA}} \quad (2.3.2.1)$$

Where, Aux represents electrical power required for auxiliary space heating (kWh); P_{HNA} represents the power consumed when the unit is not in active mode (kWh); n_j/N represents the ratio of the number of data records collected for the bin temperature (T_j)to the total number of data records in the heating season.

2.3.3 US’s specifications

ASHRAE Standard 221 (ANSI/ASHRAE, 2020). provides a method to field measure and estimate the capacity and efficiency and score the performance of an installed HVAC system. The standard applies to single-zone unitary split and packaged direct expansion cooling, air-source heat pump, and combustion furnace HVAC systems of any capacity and with forced-air distribution systems. It provides uniform methods of measurements and testing procedures for airflow, temperature, enthalpy, and power. Moreover, test instruments, specifications, and calibration requirements for capacity and efficiency measurements are specified in this standard.
The standard adopts indoor side AE difference method in field test. Test instruments include air balancing (capture) hood assembly, digital anemometer, manometers (for air pressure measurement), multisensory thermometer/psychrometer and electrical power meter. Corresponding specifications of the instruments are specified. In testing procedure, air balancing hood and thermal (or rotating vane) anemometer are used to measure the airflow of indoor terminal (shown as Figure 2.3.3-1). A digital thermometer or psychrometer probe is used to measure air temperature or enthalpy (shown as Figure 2.3.3-2). For the cooling system, temperature and humidity measurement are required to finish a minimum of seven readings at different locations simultaneously and displaying or recording each value, including wet-bulb and dry-bulb temperatures. For heating system, a similar requirement is specified for dry-bulb temperature measurement. Averaged values of temperature and enthalpy are used in capacity calculation.

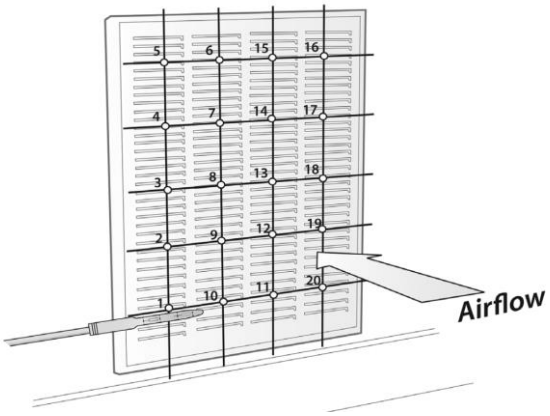

Figure 2.3.3-1. Airflow measurement procedure

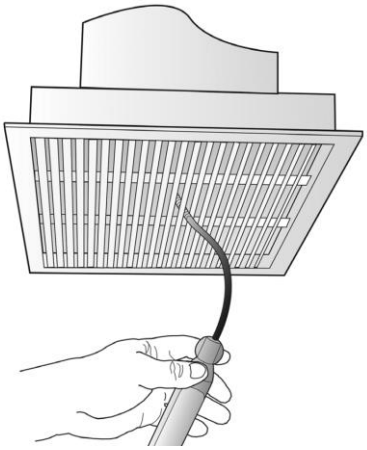

Figure 2.3.3-2. Air temperature or enthalpy measurement procedure

Based on the tested cooling or heating capacity as well as electrical consumption, the standard provides calculation method for system efficiency scoring indexes. Installed cooling system EER (ICS-eer) and installed cooling System COP (ICS-cop) represent the ratio of the total capacity delivered through the supply registers and return grilles divided into the measured total power consumed by the system and normalised to standard rating conditions.

2.3.4 Europe's specifications

For the air-to-air unit, Finnish standards NT VVS 115 (NORDTEST, 1997a) and NT VVS 116 (NORDTEST, 1997b) specify the working conditions and measurement methods for on-site performance measurement of air-to-air units, including the measurement of the compressor suction and discharge temperature and pressure, condenser outlet temperature and compressor power. The performance data of the heat pump are obtained by CEC method. Figure 2.3.4-1 shows the symbols used to define the refrigerant states which are necessary to calculate performance data. Figure 2.3.4-2 presents the basic principle of CEC method, and the heat losses were expressed as a fraction of the power input to the compressor in NT VVS 116.

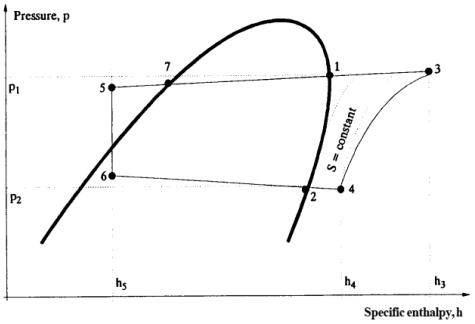

Figure 2.3.4-1. Designation of refrigerant states

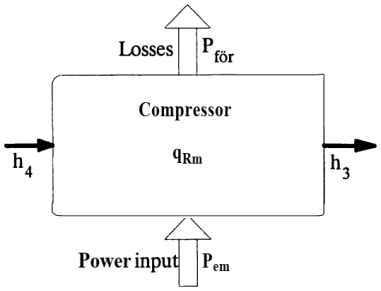

Figure 2.3.4-2. Thermal balance of the compressor

2.4 Existing data on monitored energy efficiency of heat pump systems and comparison with laboratory test results

2.4.1 Case 1 (VRF)

To investigate the actual performance parameters of the VRF system, Zhang (Zhang, 2020) measured the cooling capacities of 6 VRF systems in a building in Hefei, China (VRF S1/S2/S4/S5S6 identical with a 16 kW capacity, VRF S3 is different with a 12.5 kW capacity). During the 90-day testing period, the average daily cooling capacity of 6 VRF systems is distributed within 1.4~6.6MJ/(d·m^2). Among the 6 VRFs, S5 VRF shows the largest daily average cooling capacity because it operated for 702 h during the measurement period, as shown in Figure 2.4.1-1. In addition, the cumulative operation time of S2 VRF, with the smallest daily average cooling capacity, is about 164h. In addition, the hourly average cooling capacity of S1 and S5 VRF is higher than the corresponding rated capacity, indicating that the actual load of the rooms of the two systems could be higher than the designed load.

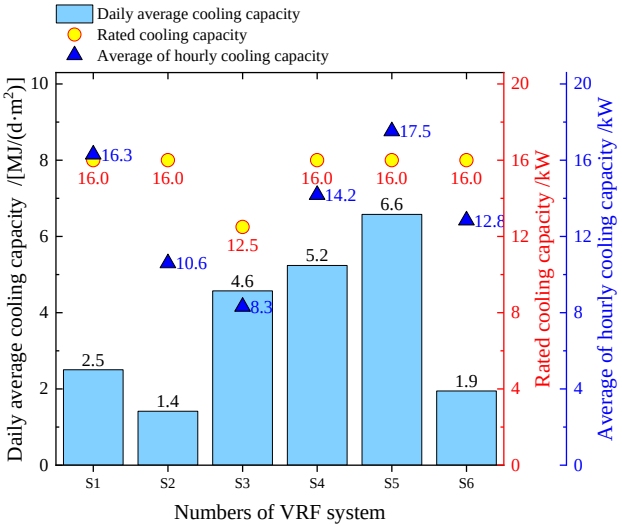

Figure 2.4.1-1. Cooling capacities of 6 VRF system

Figure 2.4.1-2 shows the statistical results of operation hours of the 6 VRFs at different part load rate during the testing period, and the result show different distribution patterns. In the field test, the periods when the part load rate of S1, S4 and S5 VRF is higher than 0.8 accounted for approximately 86%, 74% and 94%, respectively. Moreover, the part load rate of S3 VRF concentrates between 0.4 and 0.8, which accounts for approximately 87% of the total operation hours. For S2 and S6 VRF, the system operates at a relatively wide range of part load rates. Thus, the distribution pattern of operation hours on part load rate indicates that the actual operation conditions and performance of VRFs could be quite different. In addition, more attention should be paid to system design and sizing to ensure that the system operates in an appropriate and efficient part load rate area.

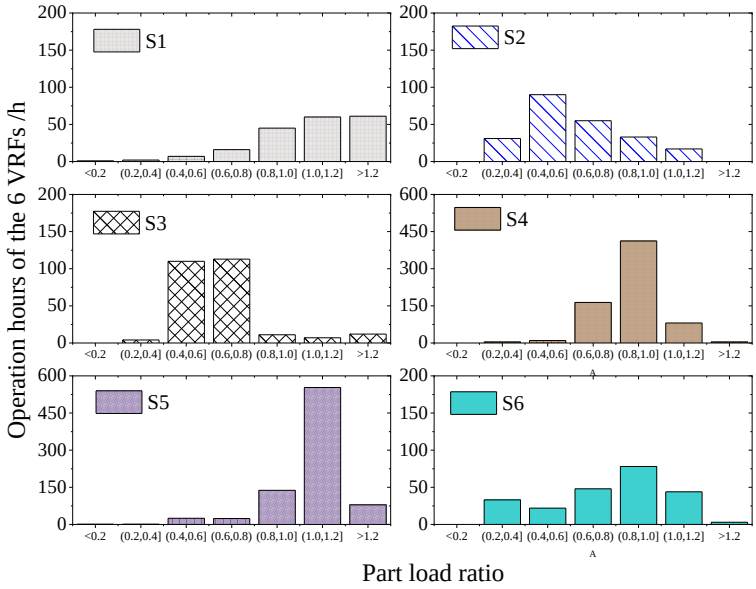

Figure 2.4.1-2. Part load rate and operation hours of the 6 VRFs

Table 2.4.1-1 shows the actual cooling operating parameters of the monitored VRF. The average power consumption of the six VRFs during the 90-day monitoring period ranged from 2.0 kW to 5.0 kW. Meanwhile, EERs were distributed in the range from 3.41 kWh/kWh to 4.08 kWh/kWh. Moreover, the average part load rate of S1 and S5 is higher than 1.0.

Table 2.4.1-1. Actual operating parameter of monitored VRFs

System code	S1	S2	S3	S4	S5	S6
Average outdoor DBT /°C	34.6	33.4	35.1	34.5	34.4	35.1
Average indoor DBT /°C	25.1	27.3	27.3	25.7	24.6	26.1
Average outdoor WBT /°C	20.2	21.4	20.9	21.5	20.3	21.3
Number of IUs	3	3	3	4	4	3
Main pipe length /m	14.7	29.7	24.1	41.7	9.7	9.7
Average power consumption /kW	4.5	2.7	2.0	4.2	5.0	3.4
Average cooling capacity /kW	16.3	10.6	8.3	14.2	17.5	12.8
Average part load rate /(kWh/kWh)	1.03	0.66	0.53	0.89	1.09	0.81
EER during testing period /(kWh/kWh)	3.66	3.98	4.08	3.41	3.49	3.75

2.4.2 Case 2 (VRF)

As part of Japan’s Ministry of the Environment's CO_2 reduction project in Japan, a nationwide field test of VRF systems was conducted in 2018 at 15 locations. The VRF units used for the tests were all products from the same manufacturer, with a rated COP in the range of approximately 4.1 to 4.3 (in cooling operation). These field tests were conducted in the country’s northern region (cold climate) and the central region (temperate climate). Data collection for analysis was performed using a newly developed device shown in Figure 2.4.2-1. This device sends operational data from the outdoor unit's control panel to a cloud server. On the cloud server, real-time calculations of VRF performance and other metrics are performed based on the transmitted data. The main analysis results related to the energy performance of VRF are as follows.

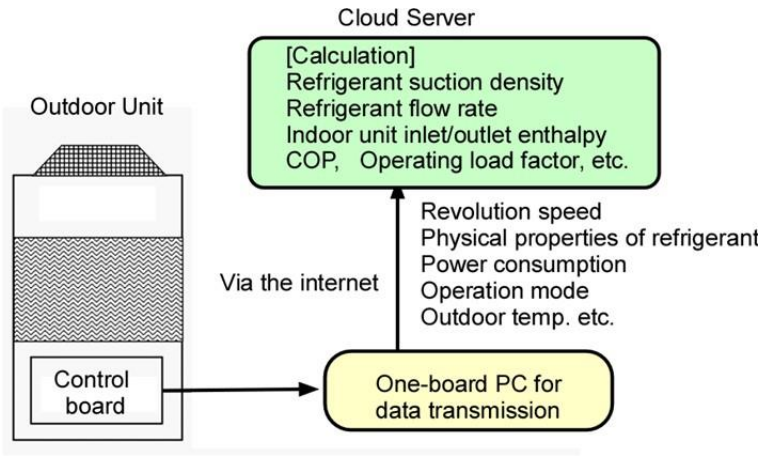

Figure 2.4.2-1. Data collection device

Table 2.4.2-1 shows the climate zone-specific average COP and average load ratio (actual capacity /nominal capacity) during heating and cooling in the field tests. The average load ratios are low, especially in the northern area (cold climate) where it is 19.6%, indicating prolonged low-load operation due to oversized equipment capacity. Generally, VRF systems are designed to achieve peak efficiency at load ratios approximately 50% to 60%, so inefficient operation at low load ranges decreases in COP.

Table 2.4.2-1. Average load ratio and COP

	Northern Area		Central Area	
Operation	Cooling	Heating	Cooling	Heating
Ave. Load ratio (%)	22.3	19.6	33.6	23.8
Av. COP	2.4	1.7	2.9	1.9
Rated COP ratio (%)	58.5	41.5	70.7	46.3

As in Figure 2.4.2-2, when outdoor units are installed nearby, the exhaust heat from the condenser of Unit B can reach the neighbouring outdoor unit (A), causing a decrease in its COP. With a temperature difference of 20°C between the exhaust and outdoor air temperature, the COP decreases by approximately 21%. As a countermeasure, installing a shielding panel between Unit A and Unit B eliminates the interference of exhaust heat, making the COP of Unit A almost equivalent to that of Unit B.

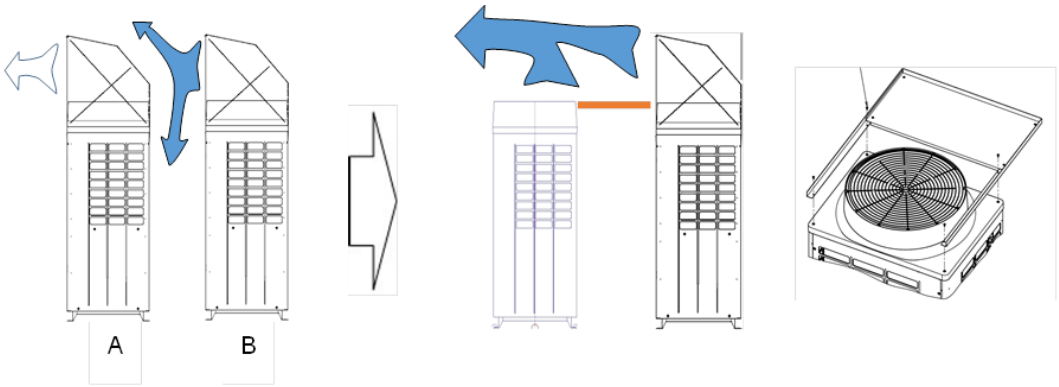

Figure 2.4.2-2. Impact of Exhaust Heat Short-circuit

The behaviour, power consumption, indoor unit suction air temperature, outside temperature, and COP values during defrost operation in winter heating are illustrated in Figure 2.4.2-3. Power consumption sharply increases at the onset of defrost operation, temporarily reaching approximately twice the rated power consumption. Defrost operation occurs at a frequency of approximately once every two hours after the start of operation. When defrost operation is performed, the average COP value for the same day is typically reduced by approximately 55% compared to normal operation.

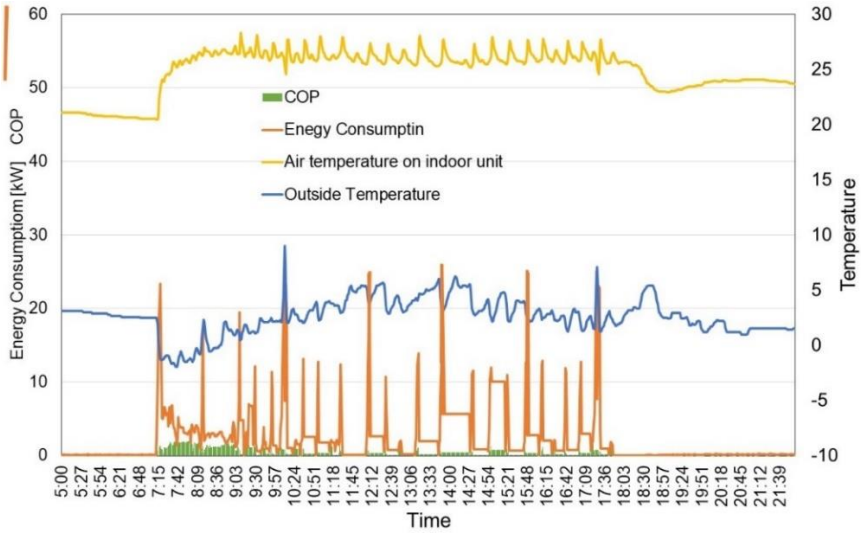

Figure 2.4.2-3. Defrost during heating operation

Since VRF has multiple indoor units connected to one outdoor unit, it accommodates the capacity demands of indoor units with lower set temperatures. Therefore, energy consumption increases compared to when set temperatures are uniform (Figure 2.4.2-4). Table 2.4.2-2 compares average set temperatures, standard deviation, average COP values, and average power consumption per unit of time in both states. The variation in set temperatures leads to a decrease in average COP and an increase in energy consumption by approximately 9%.

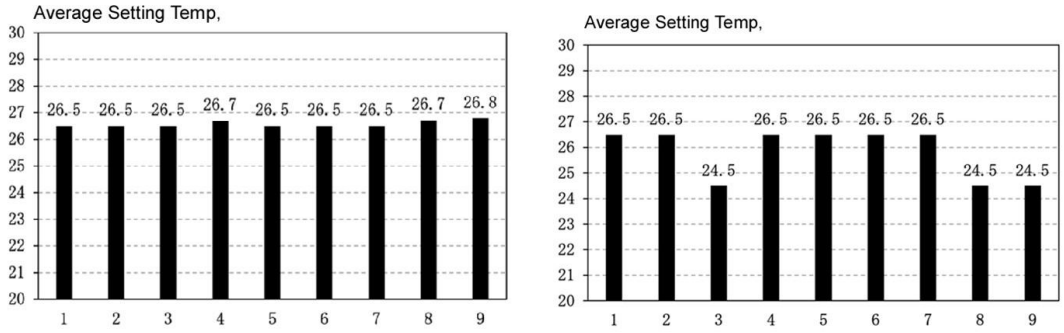

Figure 2.4.2-4. Condition of Indoor Unit Set Temperatures

Table 2.4.2-2. Impact of Variations in Set Temperatures of Indoor Units

Set Temp Condition	Average Set Temp [°C]	Standard Deviation [°C]	Average COP	Percentage change of energy use [%]
Uniform	26.7	0.11	2.54	-
Non-uniform	25.6	0.94	2.26	+8.9

2.4.3 Case 3 (RAC)

A follow-up project was carried out in 2011 (Building Research Institute, 2011)the project, three major Japanese manufacturers of RACs and a Japanese public testing laboratory (JATL: Japan Air Conditioning and Refrigeration Testing Laboratory) actively joined the dedicated team and provided technical support for measurements that were as accurate and transparent as possible. Four types of RACs were dealt with in the project. Before the field monitoring, the characteristics of the four RACs, especially the relationship between fan frequencies and airflow rates, were tested using the JATL test facility.

For cooling, the frequencies of appearance of the partial load ratio and COP for each range of the partial load ratio are shown in Figure 2.4.3-1. Seasonal average COPs written in the figure are the ratios of the

total cooling or heating load, which was dealt with by RACs when switched on to the total electricity consumption.

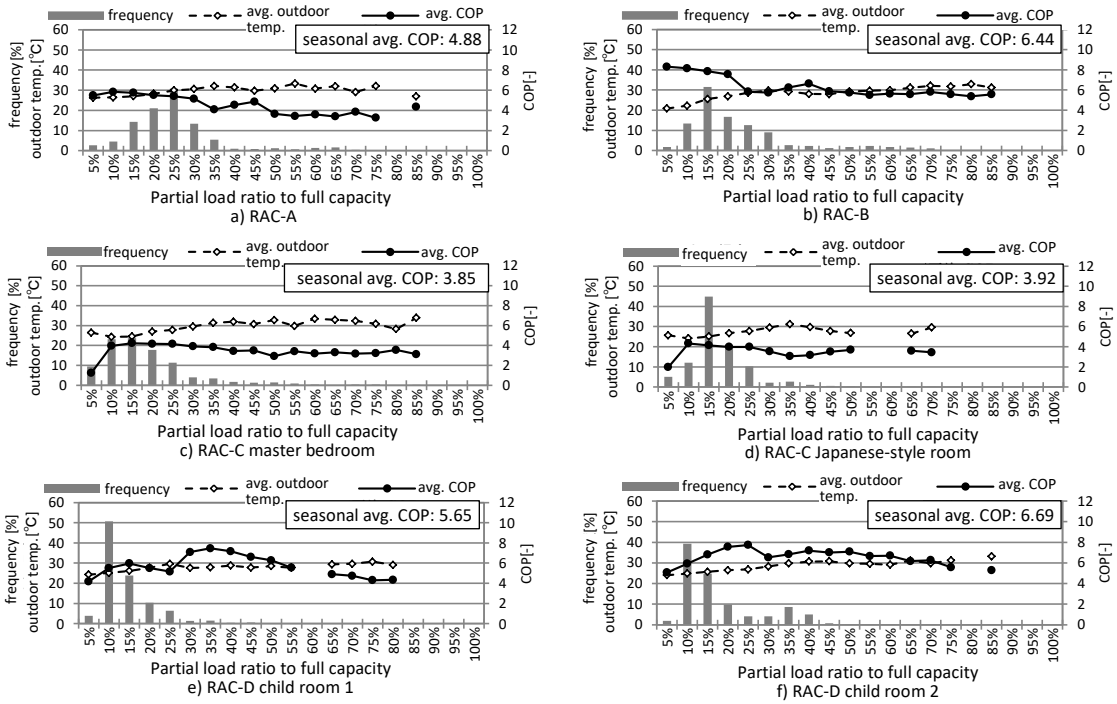

Figure 2.4.3-1. Frequencies of appearance of partial load ratio and COP for each range of the partial load ratio (Cooling)

RAC-A and RAC-B were installed side by side in the living room and were operated alternately every two weeks. The average outdoor temperatures for RAC-A and RAC-B were 29.2 °C and 26.6 °C, respectively. The peak range of appearance of the partial load ratio for RAC-A was 25%, while one for RAC-B was only 15%. For other RACs, frequencies of partial load ratio between 10% and 15% were higher than other ranges, and the actual partial load ratio for RACs used for cooling in a typical Japanese detached house needed to be very low.

On the other hand, the average COP for every 15 minutes under a partial load ratio below 25% was as high as or even higher than one under a partial load ratio above 50%. The COP of RAC-B below the partial load ratio of 20% was especially high, presumably due to lower outdoor temperature.

Figure 2.4.3.2 shows the relationship between partial load ratio and COP for different outdoor temperature ranges for cooling. In the figure, COPs for full capacity, rated capacity, and middle capacity are also plotted. There is a general tendency for COP to decrease under the partial load ratio between 0% and 20% for all monitored RACs. However, for RACs with larger capacity, such as RAC-A and RAC-B, COP could be maintained at the same level, above 20%, even below the partial load ratio of 5%. If the test result of COP for middle capacity (under 35 °C outdoor temperature) is compared with the monitored the actual COP for RAC-A, the actual COP under 33±1.5 °C and 36±1.5 °C outdoor temperature was approximately 30% lower than the test result for the middle capacity. For RAC-C in the second living room and in the main bedroom, the actual COP was approximately 50% lower than the COP for middle capacity, even though actual indoor temperature in those rooms with RAC-C was around 24 °C, which was lower than the set-point temperature for cooling (26 °C) presumably due to the characteristics of the products used in the monitoring. On the contrary, for RAC-D in child room 1, the actual COP under 30±1.5 °C outdoor temperature was only slightly higher than the COP for middle capacity. For RAC-D in child room 2, the actual COP under 33±1.5 °C was almost the same for middle capacity. Therefore, it can be said that the test result for middle capacity (with compressor frequency fixed) of RAC-D could represent actual COP in the monitoring.

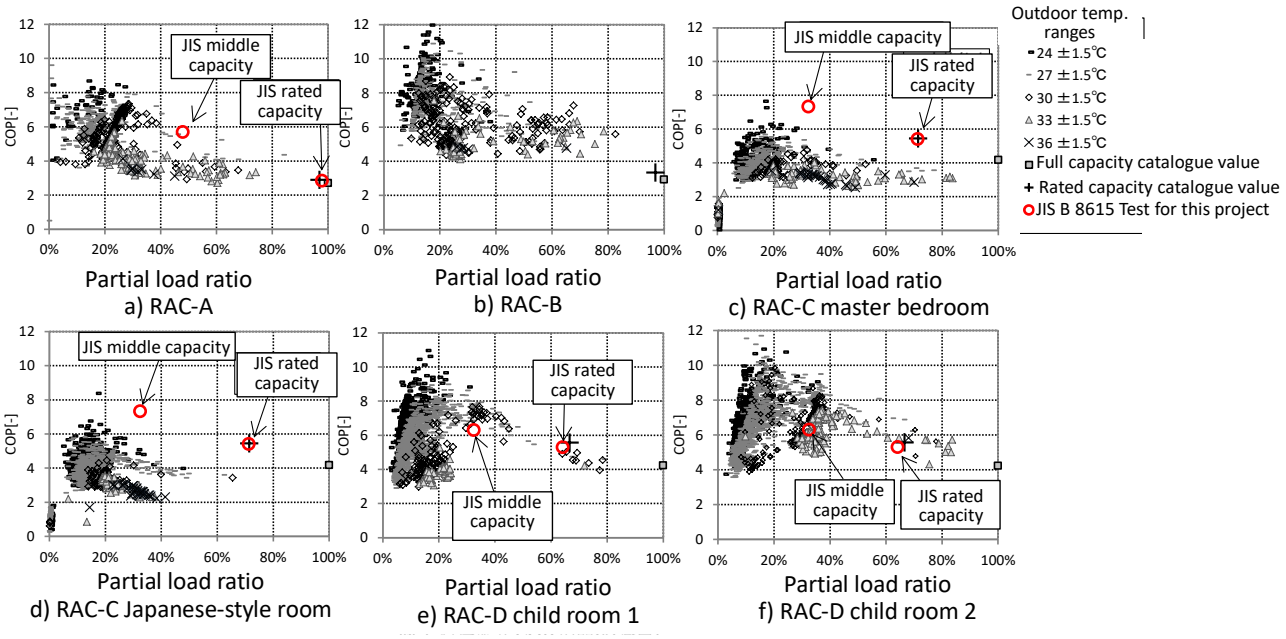

Figure 2.4.3-2. Relationship between partial load ratio and COP for different ranges of outdoor temperature for monitored five RACs (Cooling)

2.4.4 Case 4 (Water-water HP)

For smaller heat pump systems, such as room air conditioners and VRF systems, establishing measurement systems for field monitoring is feasible. However, if the capacity of a monitoring target is several hundred kW or larger, it is not realistic to install additional water flow meters and temperature sensors in existing target systems. However, many large-scale buildings (i.e., 30,000 m^2 floor area) usually have their building energy management systems (BEMS) with sensors and data logging systems, and there is a possibility to obtain support from relevant stakeholders, namely building owners, HVAC designers, installers of HVAC systems and manufacturers of control systems.

The following case (Ueno et al., 2022, Ueno, 2022) is an office building with a 32,000 m^2 gloss floor in Tokyo. In this case, the primary motivation of the building owner and the HVAC designers was to engage experts from third parties with neutral standpoints when they evaluated improvements in the energy performance of the building after the energy retrofit, including the replacement of heat and cold sources. Another important factor for successful monitoring and analysis is the reliability of BEMS and that it is carefully designed, installed, and maintained. It is not always possible to use this kind of useful BEMS when we try to analyse the behaviour of HVAC systems, including the characteristics of heat pump systems.

Figure 2.4.4-1 shows the configuration, including those generators and primary water circuits. Figure 2.4.4-2 shows monthly energy consumption for different system components, where energy consumption for heat sources is shown in the blue part at the bottom of each monthly bar.

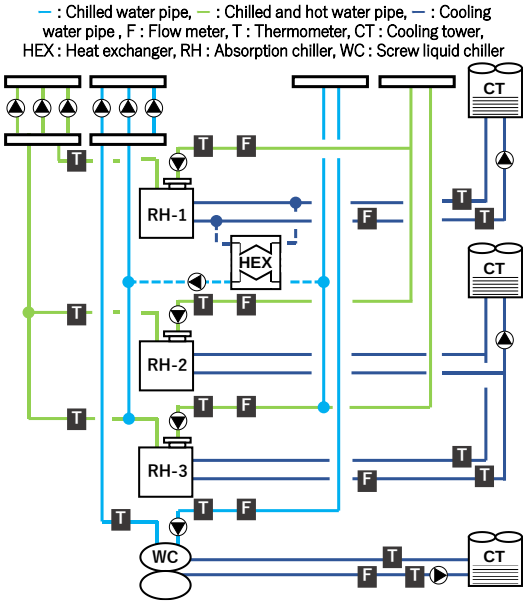

Figure 2.4.4-1. Configuration of heat and cold generators and primary hot and cold water circuit, etc.

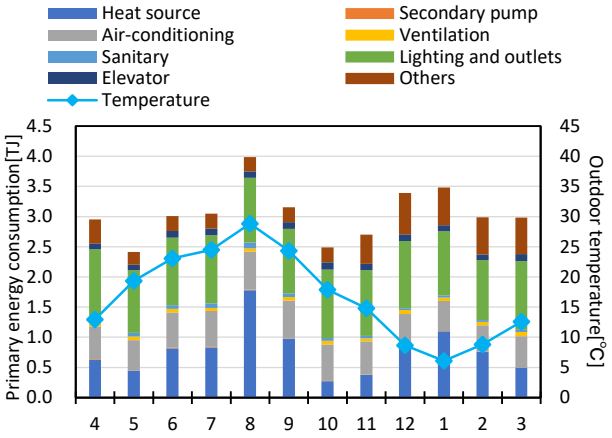

Figure 2.4.4-2. Monthly energy consumption for different components of the energy system

Figure 2.4.4-3 shows the total cooling capacity supplied by the cold sources in the middle season (May) and in the summer season (August). The annual peak of the total hourly cooling load appeared at 9 AM on the day shown as a representative of the summer season in Figure 2.4.4-3. In both seasons, the maximum hourly cooling load appeared at the beginning of the daily operation of the HVAC system. To cope with the cooling load, a screw chiller ('WC' in Figure 2.4.4-1) was primarily operated, and the screw chiller dealt with 58.1 % of the total annual cooling load. Figure 2.4.4-4 shows the cooling load dealt with by each cold generator and cold generator system's COP (primary energy basis with 9760 kJ/kWh and 1 kJ/kJ as primary energy conversion factors for electricity and city gas, respectively) during the same week shown in the previous figure. The cooling load dealt with by each cold generator is calculated by multiplying the temperature difference between the inlet and outlet water temperature and the water flow rate.

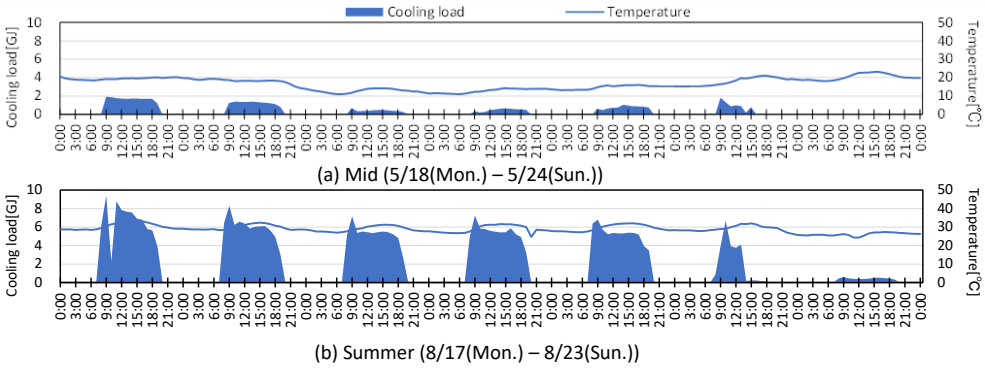

Figure 2.4.4-3. Total cooling load dealt with by the cold generators in a middle season (May) and in a summer season (August)

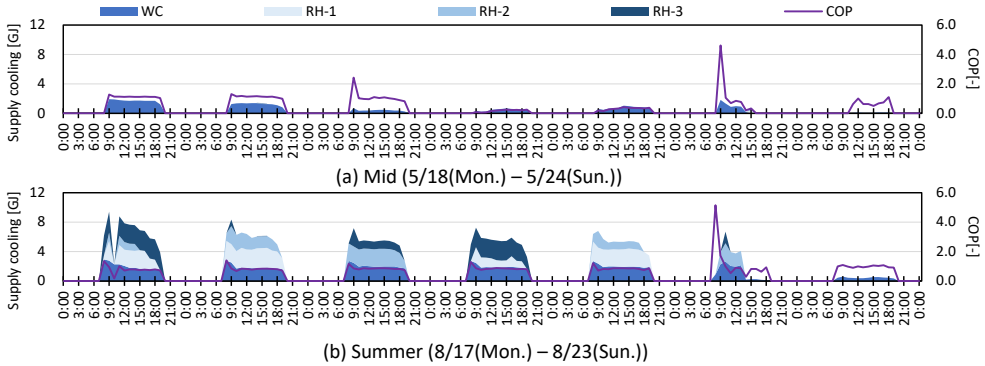

Figure 2.4.4-4. Cooling load dealt with by each cold generator and cold generator system's COP

Figure 2.4.4-5 shows the relationship between COP (primary energy basis) and part load ratio. The data in the figure includes the statuses of the cold sources under different conditions for temperatures of inlet/outlet and cooling water. It is important to notice orange dots, which are predicted COP according to the characteristic curves (as shown in Figure 3.3.4-5 in Chapter 3 in this report) prescribed for BECS's energy use calculation. The rated COPs on a primary energy basis for the two kinds of cold sources are 1.37 for the screw chiller and 1.05 for the absorption chiller system ('RH1', 'RH2', 'RH3' in Figure 2.4.4-1). The difference between predicted COPs around the partial load ratio of 1 and the rated COPs is the usage of so-called adjustment coefficients for capacity (0.95) and input energy (1.2), prescribed for BECS.

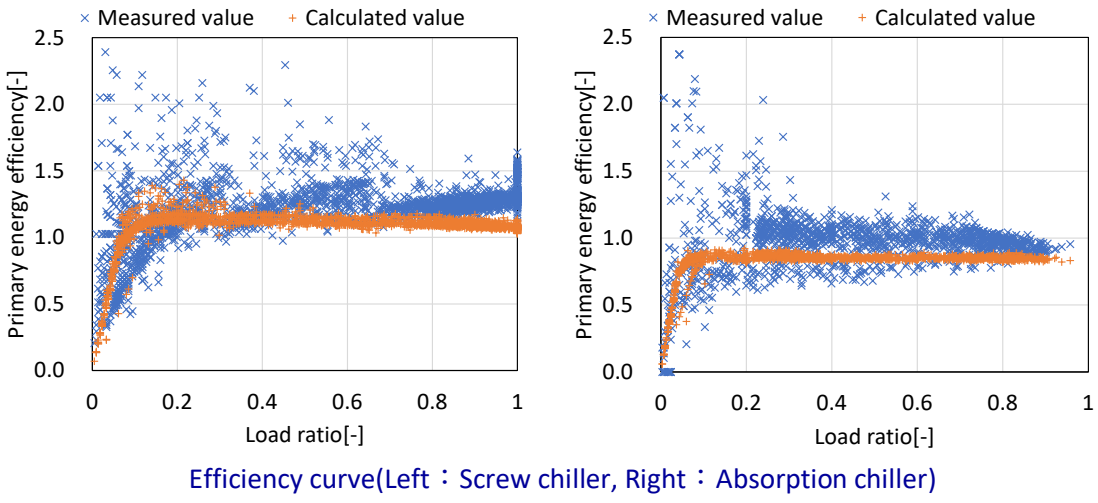

Figure 2.4.4-5. Relationship between COP (primary energy basis) and partial load ratio

2.4.5 Case 5 (Water-water HP)

To study the operational efficiency of a MBC-HP (magnetic bearing variable-speed centrifugal heat pump), Deng et al. (Deng et al., 2023) conduct field test on a practical project. As shown in Figure 2.4.5-1, a MBC-HP was applied in a heat exchange station in a municipal central heating system. Where the evaporator-side water of MBC-HP extracted heat from the return water of the primary central heating network through heat exchangers. To decrease the return water temperature of the primary central heating network to increase the heating supply ability of the district heating system, but also reduce water transport energy consumption by increasing the supply and return water temperature difference. Then the MBC-HP supplied heat to the secondary heating network for space heating.

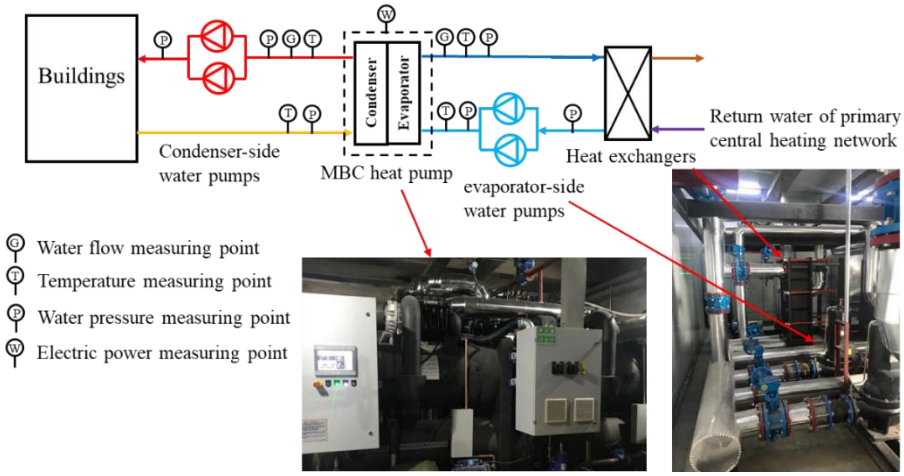

Figure 2.4.5-1. Schematic diagram of the MBC-HP system

Figure 2.4.5-2 shows the hourly heating load of the project, the maximum heating capacity of MBC-HP reached 1004.3 kW with a partial load ratio of 95.2%. Then the heating capacity gradually decreased to about 582.3 kW at the end of the heating season, with a partial load ratio of 55.2%. During 57-days operation, the average heating capacity reached 765.4 kW with an average partial load ratio of 73.0%.

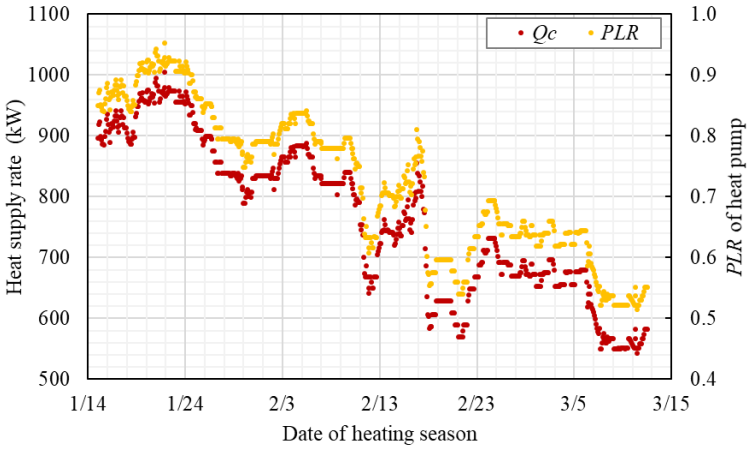

Figure 2.4.5-2. Field-test heating load and part load ratio of MBC-HP

As shown in Figure 2.4.5-3, as the MBC-HP operated in conditions with high evaporator-side water temperature, the COP_t (theoretical COP) reached higher than 9.35. And with the decreasing of $T_{c,o}$ (outlet water temperature of condenser) and increasing of outlet water temperature of evaporator, the condensing temperature decreased and evaporating temperature increased, leading to the obvious increasing of COP_t from 9.35 to 15.87. The high operational COP_t contributes to the high operational COP of MBC-HP. During the field test period, the COP varied from 7.30 to 11.18 with an average value of 8.78.

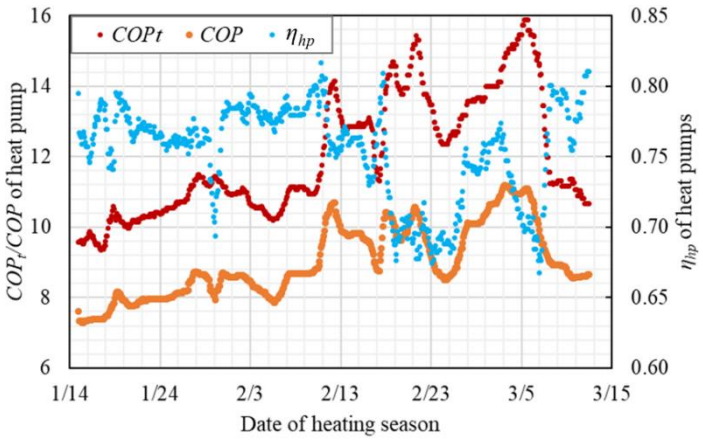

Figure 2.4.5-3. Operational energy performance of MBC-HP

Figure 2.4.5-4 depicts the influence of T_{ce} (normalised temperature difference between condensing and evaporating temperature) and partial load ratio on η_{hp} (internal efficiency of heat pumps) of MBC-HP. The results show that with T_{ce} increasing from 0.30 to 0.80, and PLR (partial load ratio) increasing from 0.40 to 1.0, the η_{hp} increases initially, then gradually decreases. Among the 57-days operation, the average η_{hp} of MBC-HP reached 0.75, with 86.7% of η_{hp} higher than 0.70, 67.5% of η_{hp} higher than 0.75, and 10.3% of η_{hp} higher than 0.78. For the rated performance of MBC-HP, the COP_t of the rated operational conditions reached 7.96. Then, with the rated COP of 5.12, the rated η_{hp} of heat pump reached 0.64. The MBC-HP has higher η_{hp} in conditions with partial PLR and T_{ce}, than the rated condition. Therefore, the MBC-HP has good regulation features, and performed efficiently in conditions with wide-range variation of heating load and compression ratio, which might fit the operation features of MD-GHPs very well.

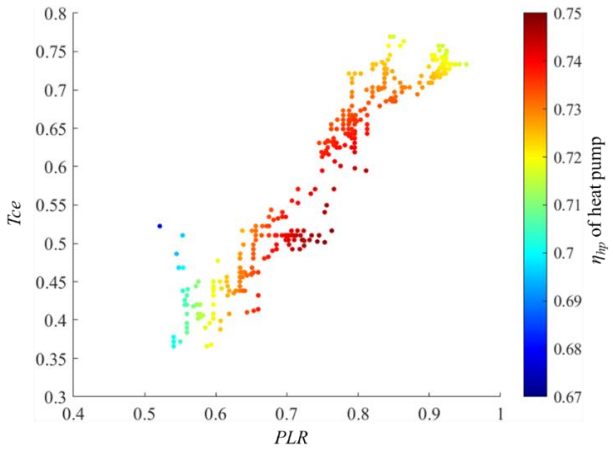

Figure 2.4.5-4. Influence of T_{ce} and PLR on η_{hp} of MBC-HP

2.4.6 Case 6 monitoring projects for air-to-water heat pumps by Fraunhofer ISE

Case 6 to Case 8 are the cases for European projects and the projects conducted in IEA Heat Pumping Technologies TCP. Relevant figures and tables can be obtained through the websites of the projects.

Two German monitoring projects are reviewed here. The first one called 'WP Efficiency' was conducted between October 2005 and September 2010 (Miara&Kramer, 2011). The project was conducted by Fraunhofer Institute for Solar Energy Systems (Fraunhofer ISE), half funded by the Federal Ministry of Economics and Technology and was supported financially and technically by seven heat pump manufacturers and two energy supply companies. The project focused on heat pumps in mainly new energy efficient (highly

insulated) residential buildings. Among systems evaluated in the project, 56 ground source to water, 18 air to water and 3 water to water heat pump systems were included. All of them were used for both space heating and domestic hot water.
As a key index, seasonal performance factor (SPF2), which is calculated as the ratio of the total outputs from a heat pump unit and a back-up heater to the total energy consumption by a fan (or a pump), a back-up heater and a heat pump unit, is used in the report. For air source heat pumps, the annual average seasonal performance factor for three years was 2.89. In the last chapter of the report, detected errors and improvement suggestions for design, installation and operation are described. The chapter touches upon the fact that lower temperature of the heat sink and higher temperature of the heat source is preferable for improving the heat pump's efficiency. It also mentions that the most efficient systems were those which charged the heating circuit directly with no buffer tank.
The second German called 'WP Monitor' was performed from December 2009 to June 2013 and was supported financially and professionally by eleven heat pump manufacturers and an energy supply company. In the report (Günther et al., 2014), mean values and distributions of annual performance values, which were calculated based on JAZ2, the same boundary mentioned above. Hot water temperatures for air-to-water systems were also reported. The average temperature of the hot water provided to the tank for space heating was in the range between 39.8 °C and 27.0 °C, while the average temperature for the domestic hot water tank was in the range between 53.2 °C and 27.0 °C (analysis for 35 air source heat pumps, Figure 32 in the report) (Günther et al., 2014).

2.4.7 Case 7 monitoring projects for air-to-water heat pumps by Eastern Swiss University of Applied Sciences

Recent results of the field measurements of heat pump systems were reported in the Annual report of the project funded by Swiss Federal Office of Energy (Prinzing et al, 2020). The field measurements were conducted by Eastern Swiss University of Applied Sciences in 23 heat pump systems (11 ground heat source systems and 12 air source systems). Only new heat pump systems that were installed mainly in a single-family home (newly built or renovated) were monitored.
Monitored heat pump systems seem to have parallel hot water circuits for domestic hot water and space heating, and they have a hot water tank only for the DHW. There was a description of the use of the electric heating element in the tank as a countermeasure for preventing Legionella disease.

2.4.8 Case 8 IEA Heat Pumping Technologies TCP projects and SEPEMO-Build

IEA HPT Annex 36 'Quality Installation / Quality Maintenance Sensitivity Studies' was launched in November 2010 and closed in November 2013 (IEA, 2014). The Annex 36 aimed at providing useful information to reduce energy usage by encouraging use of quality heat pump installation and maintenance practices to industry, policy makers and building owners/operators. It included Task 3 'Field investigation, Modelling and/or lab-controlled measurements', for which a centralised air-to-air heat pump (by French team), ten Japanese heat pump water heaters (also by French team) and a large-scale field trial of domestic heat pumps for space and water heating (by UK team) were conducted.
The outputs from the Annex 36 should be useful not only for Subtask B2 for monitoring but also for Subtask D for design guidelines, since the Annex was focused on faults to be overcome to improve energy efficiency of heat pump systems.

IEA HPT Annex 37 'Demonstration of Field Measurements of Heat Pump Systems in Buildings, Good Examples with Modern Technology' aimed at presenting examples of domestic heat pump systems with good performance (IEA, 2016). Data from 12 heat pump systems (6 ground source and 6 air source heat pumps installed in the years 2008-2012, 2 among 12 were only for space heating) in residential buildings were analysed in detail to illustrate the principles of design and installation that ensure good performance. Seasonal performance factors, SPF_{H3} and SPF_{H4} (subscripts, H3 and H4 mean boundaries when calculating

seasonal performance factors) were mainly used to express energy performance of the 12 heat pump systems.
Before the Annex 37, a preceding European project called 'SEPEMO' was conducted from 2009 to 2012 (Nordman et al., 2012). The main body of the project included 1) collection and evaluation of past and present field measurements on heat pump systems, 2) evaluation of existing methods for field measurement and calculation of seasonal performance factors, and 3) improvement and extension of existing guidelines for field measurement to include all types of heat pumps. Guidelines for heat pump field measurements were included in the deliverables from the projects (Zottl et al., 2011; Riviere et al., 2011).
IEA HPT Annex 49 'Design and Integration of heat pumps for nearly Zero Energy Buildings' was conducted from October 2016 to May 2020 with its objective for 'field monitoring of marketable and prototype heat pumps in nZEB (IEA, 2020a). In 14 nZEBs plus 3 groups of buildings including residential, office and other non-residential buildings (hotel, kindergarten, school and supermarket), especially larger buildings, monitoring wad made. The results from the monitoring projects are reported in Annex 49 Final Report Part 2 (IEA, 2020b). Only one air-source heat pump was monitored, and most targets of the monitoring were ground-source heat pumps. Several general conclusions are described in the concluding chapter, such as the recommendation of heat pumps with variable speed drive, the recommendation of natural refrigerants (e.g., propane, CO_2 and ammonia), the recommendation of utilising surplus heat at different temperature, and the recommendation of heat recovery from surplus heat sources.
IEA HPT Annex 52 'Long-term performance monitoring of GSHP systems for commercial, institutional, and multi-family buildings' was conducted from January 2018 to December 2021 with an aim to survey and create a library of quality long-term performance measurements of GSHP (Ground source heat pump) systems (IEA, 2022a). All types of sources (rock, soil, groundwater, surface water) were included in the scope. The guidelines provided by 'SEPEMO' project were refined and extended in Annex 52 and formalised in guidelines documents (IEA, 2022b; 2021a; 2021b).

2.5 Perspectives of monitoring of actual energy efficiency of heat pump systems and R&D plans in Annex 88

With the goal of energy saving and low carbon emissions, building energy management has raised great attention. As a convenient air-conditioning equipment for space cooling and heating, heat pump is widely used worldwide. To investigate the field performance of heat pumps, much research concentrates on three measurement methodologies, including the water temperature difference method, air-specific enthalpy difference (AE) method, and refrigerant-specific difference (RE) method. For water-cooled VRF, the water temperature difference method can be applied. Meanwhile, for air-to-air VRF, only AE and RE method are accessible in the field performance test. Compared with the AE method, the RE method is more suitable for long-term measurement. According to Section 2.2, field performance test technologies realise better than 25% accuracy at the current state-of-the art. Considering the technical difficulties and random operation in field tests, there are currently methods that can achieve a 10~15% relative error.
The actual performance of the heat pump was investigated by applying different field performance measurement methods in actual buildings. Actual operation characteristics were analysed by measuring and tracking heat pumps installed in actual buildings. In addition, field performance measurement methods were applied in related standards, providing feasible approaches and important indexes for performance testing, evaluation, and system retrofitting.
According to Sections 2.1 to 2.4, further promising research directions on-field performance of heat pumps may include the following five points:

(1) First, it is necessary to put more efforts into measurement accuracy improvement for all types of heat pumps in different operation conditions. Current studies rarely involve field performance measurement methods in heat recovery mode for heat recovery heat pumps. Measurement

accuracy for heat pump field performance in two-phase suction conditions and dynamic conditions remains to be improved in further studies. In addition, with the demand for individual energy management and individual billing for different terminals and occupants based on cooling/heating capacity, performance metering technology for individual indoor units should be further studied.

(2) Second, the field performance data provide basic data for related energy policies and standards studies. Through the actual performance of heat pumps, energy-efficient approaches were investigated, which promotes the construction and development of energy policies and standards.

(3) Third, energy-efficient system evaluation and design methods for heat pumps based on actual performance remain to be studied. Appropriate evaluation methods for field monitoring and lab testing remain to be studied. According to the measurement and evaluation results for the actual performance of heat pumps, problems that decrease field energy efficiency can be discovered. Thus, it is of great significance to improve actual efficiency by optimising system design and sizing methods.

(4) Fourth, further research on system control, commissioning, and management benefits from actual operation data. Better system control and management strategies that improve actual performance can be investigated. In addition, more economical cooling/heating solutions can be provided to occupants. In addition, field performance tests help determine the actual cooling/heating demand of occupants, which promotes the development of “demand-side response” energy supply conformation and proper consumption of renewable energy in the future. Devices that instantly measure the performance of heat pumps serve as an alternative to heat load sensors in buildings (Heat pump output = Building heat load). By clarifying the relationship between fluctuations in indoor heat load and the heat pump output, it becomes possible to identify the amount of energy saved through various energy-saving measures. This enables the development of precise tuning techniques related to improved energy efficiency.

(5) Fifth, if users can easily understand the performance and operational status of a heat pump system, it contributes to the improvement of the system by identifying areas for enhancement. For example, in automobiles, installing a globally standardised On-Board Diagnostics (OBD) system is mandatory, allowing relatively straightforward monitoring of operational conditions in various components and facilitating the identification of faults. In the future, it is desirable for heat pump systems also to adopt a common interface similar to OBD for improved system performance.

2.6 References for monitoring methods and database

ANSI/ASHRAE (2020). ANSI/ASHRAE Standard 221-2020. Test Method to Field-Measure and Score the Cooling and Heating Performance of an Installed Unitary HVAC System, 54 pages.

AQSIQ. (2013). The Minimum Allowable Values of the Energy Efficiency and Energy Efficiency Grades for Variable Speed Room Air Conditioners (in Chinese). Beijing.

AQSIQ. (2018). Specification for Measurement of On-Site Performance Parameters of Air Conditioner (in Chinese).

Architectural Services Department. (2007). Testing and Commissioning Procedure for Air-conditioning, Refrigeration, Ventilation and Central Monitoring & Control System Installation in Government Buildings of the Hong Kong Special Administrative Region (p. 247). The Government of the Hong Kong Special Administrative Region.

Building Research Institute (2011). Report of Committee for Actual Energy Performance of Room Air Conditioners, 28th February 2011 (in Japanese).

C.A. of B. Research (2019). Technical Specification for the Retrofitting of Multi-Connected Split Air Conditioning Systems (in Chinese). China.

C.A. of B. Research (2021). Performance Testing of Heating and Air-Conditioning Systems in Hot Summer and Cold Winter Zones (in Chinese). China.

Central Air Conditioning Market (2020). China Central Air Conditioning Market Summary Report, (2020) (in Chinese).

Deng, J.; Su, Y.; Peng, C.; Qiang, W.; Cai, W.; Wei, Q.; Zhang, H. (2023). How to improve the energy performance of mid-deep geothermal heat pump systems: Optimization of heat pump, system

configuration and control strategy, Energy, 285, 129537.
Enteria, N. ; Sawachi, T.; Saito, K. (2023). Variable Refrigerant Flow Systems: Advances and Applications of VRF, Springer Singapore, 2023.
Fahlén, P. (1989). Capacity Measurement on Heat Pumps - A Simplified Measuring Method. Swedish Council for Building Research, Sweden.
Chinese Standards. GB/T 27941-2011 (2011). Design and Installation Code for Multi-Split Air Conditioning (Heat Pump) System.
Günther, D.; Miara, M.; Langner, R.; Helmling, S.; Wapler, J. (2014). "WP Monitor" Field measure-ment of heat pump systems, Fraunhofer ISE, 15 July 2014 (in Germany).
Haga, Y., & Nobe, T. (2007). Accuracy Verification of Thermal Flux Sampler for Onsite Performance Evaluation of VRV System. In Proceedings of Clima 2007 WellBeing Indoors. Helsinki, Finland.
Ichikawa, T.; Yoshida, S.; Nobe, T.; Kametani, S. (2008). Running Performance of Split-type Air Conditioning Systems Installed in School and Office Buildings in Tokyo, Refrig. Air Cond. (2008) 1–8.
IEA - International Energy Agency (2014). Heat Pump Programme, Annex 36 Quality Installation / Quality Maintenance Sensitivity Analysis, Final Report.
IEA - International Energy Agency (2016). Technology Collaboration Programme on Heat Pumping Technologies (HPT TCP), Annex 37 Demonstration of Field Measurements of Heat Pump Systems in Buildings, Good Examples with Modern Technology, Final Report.
IEA - International Energy Agency (2019). The future of cooling: Opportunities for energy- efficient air conditioning.
IEA - International Energy Agency Technology (2020a). Collaboration Programme on Heat Pumping Technologies (HPT TCP), Annex 49 Design and Integration of heat pumps for nearly Zero Energy Buildings, Final Report.
IEA - International Energy Agency Technology (2020b). Collaboration Programme on Heat Pumping Technologies (HPT TCP), Annex 49 Field monitoring in nZEB with heat pump, Final Report Part2.
IEA - International Energy Agency (2021a). Technology Collaboration Programme on Heat Pumping Technologies (HPT TCP), Annex 52, Guidelines for Instrumentation and Data.
IEA - International Energy Agency (2012). Technology Collaboration Programme on Heat Pumping Technologies (HPT TCP), Annex 52, Guidelines for Calculation of Uncertainties.
IEA - International Energy Agency Technology (2022a). Collaboration Programme on Heat Pumping Technologies (HPT TCP), Annex 52 Long-term performance monitoring of GSHP systems for commercial, institutional, and multi-family buildings.
IEA - International Energy Agency Technology (2022b). Collaboration Programme on Heat Pumping Technologies (HPT TCP), Annex 52, Subtask 3 Report, Guide for analysis and reporting of GSHP system performance – system boundaries and key performance indicators (KPI).
Jactard, A.; Li, Z. (2011). Investigation of field methods for evaluation of air-to-air heat pump performance, Master´s Thesis, Sustainable Energy Systems programme, Department of Energy and Environment, Division of Building Services Engineering, Chalmers University of Technology, 102 pages.
JRAIA - Japan Refrigeration and Air Conditioning Association (2023). Annual Report, 2023. Available: https://www.jraia.or.jp/statistic/2306_aircon.pdf.
Kim, W., & Braun, J.E. (2016). Development and evaluation of virtual refrigerant mass flow sensors for fault detection and diagnostics. International Journal of Refrigeration, 63, 184–198.
Matsui, E.; Kametani, S. (2020). Development of On-Site Performance Evaluation System for Multi-Air Conditioning Units in Buildings, Journal of Air Conditioning, Heating, and Sanitary Engineering, Vol.45 No.282, pp.19-26, 2020.
Matsui, E.; Kametani, S.; Nobe, T. (2016). Accuracy Improvement of Performance Evaluation for Variable Refrigerant Flow Systems, Proceedings of ECOS, p424-432, 2016.
Miara, M., & Kramer, T. (2011). Heat Pump Efficiency Analysis and Evaluation of Heat Pump Efficiency in Real-life Conditions Abbreviated Version.
Naruhiro, S., & Shigeki, K. (2012). Study on the Development of the Performance Evaluation of VRF System Using the Volumetric Efficiency of the Compressor: Expansion of the Range of Application and Improvement of the Accuracy. In Proceedings of the Society of Heating, Air-Conditioning and Sanitary Engineers of Japan (SHASE).
Natural Resources Canada. (2022). Technical Guideline for Field Monitoring.
Nobe, T.; Haga, Y.; Nakamura, H.; Nobe, T.; Haga, Y.; Nakamura, H.; Tanaka, K.; Kiguchi, M. (2011). Probe insertion method for on-site evaluation of VRF system, Journal of Environmental Engineering (Transactions of AIJ). 76. 927-933. 10.3130/aije.76.927.
Nordman, R.; Kleefkens, O.; Riviere, P.; Nowak, T.; Zottl, A.; Arzano-Daurelle, C.; Lehmann, A.; Polyzou, O.; Karytsas, K.; Riederer, P.; Miara, M.; Lindahl, M.; Andersson, K.; Olsson, M. (2012). Seasonal Performance Factor and Monitoring for Heat Pump Systems in the Building Sector (SEPEMO-Build), Final Report.
NORDTEST (1997a). NT VVS 115 - Refrigeration and heat pump equipment: General conditions of field testing and presentation of performance, Finland, 19 pages.

NORDTEST (1997b). NT VVS 116 - Refrigator and heat pump equipment: Check-ups and performance data inferred from measurements under field conditions In the refrigerant system, Finland, 13 pages.
Prinzing, M.; Berthold, M.; Eschmann, M.; Bertsch, S. (2020). Field measurements from heat pump systems, Heating season 2019/2020, 30 September 2020, Swiss Federal Office of Energy (in Germany).
Riviere, P.; Nordman, R.; Tran, C-T.; Coevoet, M.; Zottl, A. (2011). Guidelines for heat pump field measurements on air-to-air heat pumps, SEPEMO project report.
Shimizu, S.; Haga, Y.; Yumoto, Y.; Kametani, S.; Nobe, T. (2006). Actual performance evaluation system of package air-conditioner by sampling system of heat rejection flux from outdoor unit, Part2: Accuracy verification of sampling system of heat rejection flux from outdoor unit in the calorie box, Tech. Pap. Annu. Meet. Soc. Heat. Air-Conditioning Sanit. Eng. Japan. (2006) (in Japanese).
Shimizu, S., Haga, Y., & Nobe, T. (2007). On-site Evaluation Method of Multi Split Air Conditioner System, Part 2: Investigation of Actual Efficiency by Sampling System. Journal of Asian Architecture and Building Engineering, 6(2), 341-347.
Takahashi, S., Kametani, S., Itou, M., & Funatani, A. (2008). Study on Performance Evaluation Method of a Split Air Conditioning System Based on Characteristic Curve of the Compressor Mass Flow Rate. In Proceedings of the International Refrigeration and Air Conditioning Conference. Purdue University, West Lafayette, IN, USA.
Teodorese, V., Detroux, L., & Lebrun, J. (2007). Testing of a Room Air Conditioner: High Class RAC Test Results - Medium Class RAC Test Results. University of Liege, Belgium.
Tran, C.T., Rivière, P., Marchio, D., & Arzano-Daurelle, C. (2012). Refrigerant-based measurement method of heat pump seasonal performances. International Journal of Refrigeration, 35(6), 1583–1594.
Ueno, T.; Yamazaki, Y.; Yoshida, S.; Sato, K.; Sawachi, T. (2022). Estimation for Energy Saving Effect of Chilled Water Temperature Relaxation in an Office Building with Multiple Heat Sources, Journal of Environmental Engineering, Architectural Institute of Japan, Vol. 87, No.802, December 2022 (in Japanese).
Ueno, T. (2022). BEMS Data Analysis of Heat Source Facilities in Japan, A presentation in the Second Workshop for IEA EBC Annex 88, 9th March 2022.
Won, A.; Ichikawa, T.; Yoshida, S.; Sadohara, S. (2009). Study on running performance of a split-type air conditioning system installed in the national university campus in Japan, J. Asian Archit. Build. Eng. 8 (2009) 579–583.
Xiao, H., Shi, J., Yang, Z., Wang, B., Shi, W., & Li, M. (2022). Precision improvement method for onsite performance measurement of variable refrigerant flow system. Building and Environment, 2022, 108626, ISSN 0360-1323, https://doi.org/10.1016/j.buildenv.2021.108626.
Yang, Z., Ding, L., Xiao, H., Zhang, G., Wang, B., & Shi, W. (2020). All-condition measuring methods for field performance of room air conditioner. Applied Thermal Engineering, 180, 115887.
Zhang, G., Liu, W., Xiao, H., Shi, W., Wang, B., & Li, X. (2019). New method for measuring field performance of variable refrigerant flow systems based on compressor set energy conservation. Applied Thermal Engineering, 154, 530–539.
Zhang, G. (2020). Research on the measurement method for the cooling and heating capacity of the multi-split air-conditioner and its running performance in office buildings, Tsinghua University, (in Chinese).
Zhao, W. (2009). Study on Part Load Performance of Variable Refrigerant Flow System. Tsinghua University, Master's Thesis, Beijing, China.
Zottl, A.; Nordman, R.; Coevoet, M.; Riviere, P.; Miara, M.; Benou, A.; Riederer, P.; Andersson, K.; Lindahl, M. (2011). Guidelines for heat pump field measurements for hydronic heating systems, SEPEMO project report.